



Published in final edited form as:

Cell Stem Cell. 2009 March 6; 4(3): 217–225. doi:10.1016/j.stem.2009.01.016.

Syndecan-4 Expressing Muscle Progenitor Cells in the SP Engraft as Satellite Cells During Muscle Regeneration

Kathleen Kelly Tanaka^{*}, John K Hall^{*}, Andrew A Troy^{*}, DDW Cornelison[†], Susan M Majka[#], and Bradley B Olwin^{*,†}

^{*} MCD Biology, University of Colorado, Boulder, CO 80309 USA

[†] Biological Sciences and Bond Life Sciences Center, University of Missouri, Columbia, MO 65211 USA

[#] Dept of Medicine/Cardiology, University of Colorado Health Sciences Center, Aurora, CO 80045 USA

Summary

Skeletal muscle satellite cells, located between the basal lamina and plasma membrane of myofibers, are required for skeletal muscle regeneration. The capacity of satellite cells as well as other cell lineages including mesoangioblasts, mesenchymal stem cells and side population (SP) cells to contribute to muscle regeneration has complicated the identification of a satellite stem cell. We have characterized a rare subset of the muscle SP that efficiently engraft into the host satellite cell niche when transplanted into regenerating muscle, providing 75% of the satellite cell population and 30% of the myonuclear population, respectively. These cells are found in the satellite cell position, adhere to isolated myofibers, and spontaneously undergo myogenesis in culture. We propose that this subset of SP cells (satellite-SP cells) characterized by ABCG2, Syndecan-4 and Pax7 expression, constitutes a self-renewing muscle stem cell capable of generating both satellite cells and their myonuclear progeny *in vivo*.

Introduction

Maintenance and repair of skeletal muscle tissue is essential for survival of locomotor organisms. Although satellite cells are thought to be the primary source of new myonuclei during skeletal muscle growth and repair, the engraftment capability of isolated satellite cells into injured or diseased skeletal muscle is poor (Asakura et al., 2007; Montarras et al., 2005; Beauchamp et al., 1999). Indeed, cells derived from other sources including mesoangioblasts (Sampaolesi et al., 2003; Sampaolesi et al., 2006), pericytes (Dellavalle et al., 2007), and bone marrow stem cells (Gussoni et al., 1999; LaBarge and Blau, 2002) engraft into myofibers with greater efficiency than isolated satellite cells. Only a subset of muscle cells enriched for CD34 expression by cell sorting is capable of engraftment into skeletal muscle myofibers and into the host satellite cell niche (Montarras et al., 2005; Cerletti et al., 2008; Sacco et al., 2008). Although efficient at myonuclear engraftment, these cells engraft with much lower frequencies into the satellite cell niche. These observations together with data demonstrating asymmetric division of satellite cells (Kuang et al., 2007)

[†]Corresponding author: 347 UCB, MCD Biology, University of Colorado, Boulder, CO 80309, Phone: 303-492-6816, Fax: 303-492-1587, Email: Bradley.Olwin@colorado.edu.

Publisher's Disclaimer: This is a PDF file of an unedited manuscript that has been accepted for publication. As a service to our customers we are providing this early version of the manuscript. The manuscript will undergo copyediting, typesetting, and review of the resulting proof before it is published in its final citable form. Please note that during the production process errors may be discovered which could affect the content, and all legal disclaimers that apply to the journal pertain.

and satellite cell heterogeneity (Olguin and Olwin, 2004; Zammit et al., 2004) suggest that a rare population of satellite cells may exist with enhanced stem cell-like characteristics.

Many adult tissues including bone marrow (Goodell et al., 1996), heart (Asakura et al., 2002), lung (Majka et al., 2005) and skeletal muscle (Majka et al., 2003) possess cells that exhibit the SP phenotype. Indeed, the discovery of these cells in skeletal muscle and their myogenic potential suggested they may function as satellite cell progenitors; however, the low efficiency of muscle SP cell engraftment into skeletal muscle suggested that this population was not representative of a skeletal muscle progenitor (Muskiewicz et al., 2005). Here, we show that a subset of the muscle SP cells that possess both SP and satellite cell characteristics function as efficient satellite cell progenitors. Although the majority of SP cells reside in the interstitium (Meese et al., 2004), satellite-SP cells: (i) can be found in the satellite cell position, (ii) remain associated with isolated myofibers, (iii) spontaneously fuse in culture and, (iv) generate satellite cell progeny *in vivo*, all characteristics consistent with a satellite cell progenitor. Evidence that a subpopulation of satellite cells may function as a reserve or progenitor population was described using *in vivo* labeling techniques over three decades ago (Schultz, 1996). Recently, the demonstrations of satellite cell heterogeneity (Olguin and Olwin, 2004; Zammit et al., 2004) coupled with identity of a small population of satellite cells that exhibits asymmetric cell division (Kuang et al., 2007), and long term BrdU retention (Shinin et al., 2006), all characteristics of stem cells, has further strengthened this idea.

Skeletal muscle SP cells express Syndecan-3 and Syndecan-4

When examining data from microarray analyses of FACS (fluorescent activated cell sorting) sorted Syndecan-3+/Syndecan-4+ cells isolated from uninjured muscle we found high-level expression of both *Abcg2* and *Cd34*. This expression is dramatically reduced in cells sorted from BaCl₂-injured muscles, 24hr post-injury (Fig. 1A, Supplemental Table 1). The high level expression of these cell markers coupled with their differential expression following injury prompted us to examine ABCG2 and CD34 protein expression in the satellite cell population. Although others have successfully observed CD34 immunoreactivity in satellite cells, in our hands the staining patterns were highly variable and inconsistent (data not shown) and thus, we focused on ABCG2.

ABCG2 is the ATP binding cassette transporter responsible for the majority of the SP phenotype originally characterized in bone marrow (Goodell et al., 1996; Zhou et al., 2001). Therefore, we asked if skeletal muscle cells expressing Syndecan-4, which marks all Pax7+ and c-met+ satellite cells (Cornelison et al., 2001; Brack et al., 2007; Bosnakovski et al., 2008) also express ABCG2 protein using an anti-ABCG2 antibody. First, to verify that the anti-ABCG2 antibody identifies cells exhibiting the SP phenotype, we performed FACS analysis of bone marrow cells using Hoechst 33342 dye efflux to identify SP cells (R3 in Fig. 1B, C) and compared the SP cells identified by dye efflux with those identified by anti-ABCG2 immunoreactivity. ABCG2 immunoreactive cells comprised 90–95% of the SP cell population confirming the utility of the ABCG2 antibody for identifying SP cells (Fig. 1D). Although the majority of bone marrow SP cells are ABCG2+, multiple ABC transporters contribute to the SP phenotype and thus, the entire SP is not ABCG2 immunoreactive (Zhou et al., 2001). In hindlimb skeletal muscle we identified SP cells by dye efflux that comprised 1–5% of total hindlimb cells (Fig. 1E, F, R3 region) similar to that reported by others (Montanaro et al., 2004). The majority (90%) of these SP cells are ABCG2 immunoreactive (Fig. 1G, grey). To further verify the utility of the ABCG2 antibody, we examined cells located above the SP gate in the main population, which are generally not ABCG2 immunoreactive (Fig. 1G, hatched). Finally, we isolated SP cells using Hoescht dye exclusion from a mouse expressing GFP from an IRES-GFP knocked into the 3rd intron of the *Abcg2* locus (Tadjali et al., 2006). These cells are both GFP+ and anti-GFP

immunoreactive, confirming that the anti-ABCG2 antibody recognizes cells expressing *Abcg2* (Fig. 1H). We then examined muscle SP cells isolated by dye exclusion for satellite cell markers by FACS and found that 5–10% of hindlimb SP cells are immunoreactive for the satellite cell markers Syndecan-3 and Syndecan-4 (Fig. 1I). This subset of hindlimb cells represented in the Venn Diagram is a subfraction of the SP that express the satellite cell marker Syndecan-4 (Fig. 1J). To allow detection of additional markers and to alleviate the damaging effects of the Hoescht 33342 dye, we used anti-ABCG2 immunoreactivity to identify and isolate muscle SP cells except where noted.

A subset of satellite cells is SP cells

To further characterize the Syndecan-3+/Syndecan-4+ SP cells we analyzed mononuclear cells from mouse hindlimb muscle tissue by FACS using the anti-ABCG2 antibody. Of the entire population of mononuclear cells in the hindlimb, (Fig. 2A), 10–20% are Syndecan-4 immunoreactive (Fig. 2B) and all Syndecan-4+ cells are viable (Fig. 2C). To verify that these cells are not significantly contaminated by cells from the blood and endothelial lineages, we profiled for CD45, Gr-1, Mac-1, Thy-1 and PECAM-1. The blood cell markers were not expressed by Syndecan-4+ cells isolated from skeletal muscle (Fig. 2D-G). Prior reports suggest that satellite cells as well as endothelial cells express PECAM-1 (CD31) (De Angelis et al., 1999), and we found a similar small percentage of Syndecan-4+ cells (7% of all Syndecan-4+ cells) and Syndecan-4+/ABCG2+ cells (8% of all dually positive satellite cells) express PECAM-1 (Fig. 2H, Supplemental Fig. 1). We then profiled for three markers simultaneously, Syndecan-4, ABCG2 and Sca1, another stem cell marker previously identified on SP cells (Asakura et al., 2002; Jackson et al., 1999; Mitchell et al., 2005). As expected, the majority of ABCG2+ cells and Sca1+ cells are Syndecan-4 negative (Fig. 2I, R10 and 2J, R14 respectively). Consistent with the SP cell data (see Fig. 1), we found that a population of Syndecan-4+ cells is immunoreactive for ABCG2 (Fig. 2I, R11) and for Sca1 (Fig. 2J, R15). The majority of ABCG2+ cells appear Sca1+ (Fig. 2K, R19) and this ABCG2+/Sca1+ population is enriched in the ABCG2+/Syndecan-4+ cell population where virtually all Syndecan-4+/ABCG2+ cells are Sca1+ (Fig. 2L R19 compared to R21) and half of the Syndecan-4+/Sca1+ cells are ABCG2+ (Fig. 2L, R18 compared to R19). This subset of satellite cells is rare, comprising 0.25% of the entire hindlimb mononuclear cell population (Fig. 2Q) and averages between 3 and 10% of the Syndecan-4+ satellite cell population.

If these ABCG2+/Sca1+/Syndecan-4+ cells are satellite cells, they should reside in the satellite cell position in muscle sections and be retained on intact myofibers following myofiber isolation by enzymatic digestion. We found rare cells in the satellite cell position underneath the basal lamina (Fig. 2M, inset) immunoreactive for Syndecan-4 and ABCG2 (Fig. 2N-P, inset). Some of these cells were found tightly associated with freshly isolated myofibers (Fig. 2R-U, carets). Although the percentages from the FACS profiles suggest that 1–2 Syndecan-4+/ABCG2+ SP cells are present on a typical myofiber (assuming ~25 satellite cells per myofiber), when fixed and stained we detect fewer cells than expected (0.5–1/myofiber) likely due to the low expression of ABCG2. These cells were also Sca1+ (Fig. 2S, caret), strongly suggesting that they represent the cells observed by flow cytometry. Because these cells are present at the satellite cell position in skeletal muscle tissue, are found in the SP, express satellite cell markers and remain tightly associated with myofibers during enzymatic isolation, we propose that these cells represent a subset of satellite cells and refer to this population as satellite-SP cells.

Satellite-SP cells express Pax7 and have distinct behavior in culture

The presence of satellite-SP cells on intact myofibers allows independent analysis of their behavior and comparison with the general satellite cell population in culture. Distinct from

the major Syndecan-4+ population where clusters of cells appear following 6d in culture, single satellite-SP cells appear surrounded by Syndecan-4+ satellite cells (Fig. 3A, B, caret marks satellite-SP cell). A number of possibilities could explain this observation including: (i) asymmetric cell division, (ii) very slow cell cycling, (iii) enhanced migration of the satellite-SP cells off of the myofibers, (iv) enhanced cell death of satellite-SP cells or, (v) a failure of satellite-SP cells to divide in culture. The first two possibilities are not likely as we did not observe satellite-SP cells on the tissue culture plates adjacent to the myofibers nor did we observe apoptosis of satellite cells (data not shown). It is also possible that the ABCG2 immunoreactivity is lost during culture and we cannot directly assess this possibility. To demonstrate cell cycle entry of satellite-SP cells we employed a BrdU pulse chase assay, where myofibers were cultured for the first 48hr after harvest in the presence of BrdU followed by either a 48hr or a 6d chase in the absence of BrdU. Typically, Syndecan-4+ satellite cells on intact myofibers in culture will begin DNA synthesis 8–12hr following isolation and undergo a synchronous division between 36 and 45hr with subsequent cell divisions occurring much more rapidly at 10–12hr (unpublished data). All satellite cells (Fig. 3C–F, arrows) and satellite-SP cells (Fig. 3C–F, carets) incorporate BrdU during the first 48hr in culture and retain label 48hr later, indicating that satellite-SP cells undergo a first cell division with kinetics roughly similar to Syndecan-4+ cells. However, following a 6 day chase in the absence of BrdU Syndecan-4+ satellite cells continue to proliferate and dilute the BrdU label (Fig. 3G–J, arrows), whereas all satellite-SP cells retain BrdU, indicating that these cells cease cell division or cycle very slowly (Fig. 3G–J, caret). Curiously, we rarely observe ABCG2+/Syndecan-4+ doublets and typically find single isolated cells (Figs. 3A–J). If this is the result of asymmetric satellite-SP cell division giving rise to one daughter cells that retains the parental phenotype, the other daughter would be predicted to proliferate and thereby dilute the BrdU label. This is a possibility since rare, asymmetric division of satellite cells has been observed (Kuang et al., 2007) and the expression of stem cell markers by the satellite-SP cells suggests that an asymmetric cell division event could explain the predominance of single satellite-SP cells.

To further define the satellite cell character of satellite-SP cells, we asked if they express the paired box transcription factor Pax7, which is considered a marker of quiescent satellite cells and is required for satellite cell specification *in vivo* (Seale et al., 2000). Satellite-SP cells on intact myofibers that stain positive for Syndecan-4 (Fig. 3K) and ABCG2 (Fig. 3L) appear Pax7+ (Fig. 3M, O). FACS sorted satellite-SP cells (Fig. 3P) were Syndecan-4+ and stained positive for Pax7 when cytopun (Supplemental Fig. 2); when analyzed by FACS, essentially all satellite-SP cells are Pax7+ (Fig. 3Q), suggesting that these cells are committed to the myogenic lineage.

Satellite-SP cells express satellite cell markers and remain associated with myofibers, but we have not determined whether these cells are capable of spontaneous myogenic differentiation. In previous reports, skeletal muscle SP cells have not exhibited this potential, and are only capable of initiating myogenesis when co-cultured with satellite cells or skeletal muscle cell lines (Asakura et al., 2002). We reasoned that if satellite-SP cells were the only SP cells capable of myogenesis, then their myogenic phenotypes may have been overlooked in culture since they represent only a small percentage of the muscle-derived SP population. Alternatively, myogenic commitment of muscle SP cells by co-culture with myogenic cell lines may represent a required community effect. Therefore, we asked if satellite-SP cells are inherently myogenic in clonal cultures. FACS sorted satellite-SP cells cultured in growth media for 5d differentiated into multinucleated myotubes (Fig. 3R), whose nuclei express MyoD (Fig. 3S) and retain mononuclear MyoD+/Pax7+ cells (Fig. 3S, T, inset). As a further test to determine if satellite-SP cells, isolated by Hoechst dye exclusion are capable of myogenesis, muscle SP cells were sorted into Syndecan-4+ and Syndecan-4– pools (Fig. 3U, V) and the pools were individually cultured for 3 weeks in

stem cell media. As expected, Syndecan-4⁻ muscle SP cells fail to commit to a myogenic lineage (Fig. 3W), while satellite-SP cells spontaneously differentiated and fused into multinucleated myotubes (Fig. 3X). Thus, when isolated from the bulk of SP cells by dye exclusion or by FACS sorting, satellite-SP cells are capable of spontaneous myogenesis, supporting the hypothesis that these cells are capable of commitment to the myogenic lineage.

Satellite-SP cells are myogenic following transplantation

If satellite-SP cells function as a myogenic progenitor or satellite stem cell then we predict that they would produce satellite cell progeny capable of incorporation into the satellite cell niche as well as contributing myonuclei to myofibers. To address both the myogenic and stem cell capabilities of satellite-SP cells compared to satellite cells we identified Syndecan-4⁺ cells by FACS from a Rosa26 (Zambrowicz et al., 1997) donor mouse to lineage mark cell progeny (Fig. 4A), then sorted the Syndecan-4⁺ cells into two separate pools (Fig. 4B), the satellite-SP cells (Syndecan-4⁺/ABCG2⁺/Sca1⁺) and satellite cells (Syndecan-4⁺/ABCG2⁻/Sca1⁻). Tibialis anterior muscles of separate host mice were injected with 2500 satellite-SP cells or 2500 satellite cells in the presence of 1.2% BaCl₂ to induce muscle regeneration. The transplanted muscles were examined for donor cell contribution 30d following induced injury. Cross sections from the satellite cell transplant show evidence of regeneration as indicated by centrally located nuclei (Fig. 4C, asterisks), but there is little detectable donor cell engraftment into the myofibers and no detectable engraftment into the satellite cell niche (Fig. 4C, data not shown). In satellite-SP transplanted muscle β-galactosidase⁺ myofibers are numerous and clearly evident (Fig. 4D, E), suggesting engraftment of donor satellite-SP cells. Moreover, β-galactosidase⁺ donor-derived cells (Fig. 4F) that express Syndecan-4 (Fig. 4G) were readily found in the host satellite cell niche located underneath the basal lamina (Fig. 4F-I), demonstrating that satellite cells as well as myonuclei can be derived from satellite-SP cell progeny *in vivo*. Satellite-SP cells contribute to myonuclei as 30% of myofibers were β-galactosidase⁺ and thus contained donor-derived nuclei (Fig. 4E, Supplemental Table 2). The majority of these fibers possessed centrally located nuclei (Fig. 4C, asterisk, Supplemental Table 2) indicative of regenerated tissue. Transplantation of satellite cells produced few or no detectable β-galactosidase⁺ fibers (Fig. 4C), however we did find centrally located nuclei (Fig. 4C, asterisk) affirming that the tissue was injured.

Engraftment of satellite-SP cells into the host tissue preferentially engrafts into the satellite cell niche as demonstrated by the striking contribution of donor satellite cells to the regenerated tissue (Fig. 4J). We found that 75% of all satellite cells present in the regenerated tibialis anterior muscle were donor-derived cells (Fig. 4J, Supplemental Table 3) as they engrafted into the satellite cell niche, were located underneath the basal lamina (Fig. 4F-I) and expressed the satellite cell marker Syndecan-4 (Fig. 4G, I). The engraftment of satellite-SP cells demonstrates they robustly and preferentially contribute to the satellite cell pool. Although we found β-galactosidase expression in myotubes, the capacity of the satellite-SP cells to differentiate into muscle *in vivo* is not addressed by these experiments. To determine if satellite-SP cells are capable of muscle differentiation, satellite-SP cells from a ROSA26 mouse were isolated by FACS as Syndecan-4⁺/ABCG2⁺/Sca1⁺ and 2500 cells injected into the tibialis anterior muscle of an *mdx*^{4^{cv}} mouse (Chapman et al., 1989) in the presence of BaCl₂ (Fig. 5A, B). An examination of muscle sections 30d following engraftment reveal extensive regeneration (Fig. 5C, asterisks mark centrally located nuclei), extensive contribution of Dystrophin from the donor cells (Fig. 5D) and localization of donor-contributed Dystrophin inside the basal lamina (Fig. 5E, F). Contribution of engrafted satellite-SP cells to the myonuclear compartment in *mdx*^{4^{CV}} was substantially greater than

wild type transplants where ~70% of the myofibers in the engrafted muscle were Dystrophin + (Fig. 5G, Supplemental Table 4).

Engraftment of satellite-SP cells differed from engraftment of freshly isolated, CD34-enriched satellite cells, which require injection into irradiated, immunodeficient *mdx* mice (Montarras et al., 2005; Muskiewicz et al., 2005; Sacco et al., 2008) or diseased (*mdx*) mice (Cerletti et al., 2008). Thus, satellite-SP cells compete effectively with endogenous satellite cells since the host tissue is not irradiated to destroy the endogenous cells and injections are successful in wild type regenerating muscle, not diseased muscle tissue, where endogenous satellite cells may be compromised. Together, our data show preferential engraftment of satellite-SP cells into the satellite cell niche with efficiencies not seen for any other cell types, suggesting the satellite-SP cell may function as a satellite stem cell. To provide further evidence in support of this hypothesis, we re-injured tibialis anterior muscles in *mdx^{4CV}* mice engrafted with 2500 satellite-SP cells from a ROSA26 mouse (Fig. 6A–C). Muscle sections were examined for the contribution of donor cells to the satellite cell and myonuclear compartments thirty days following re-injury. Similar to the primary engraftment, re-injured muscle shows extensive contribution of donor cells to the myonuclear compartment demonstrated by β -galactosidase+ myofibers (Fig. 6D). Moreover, a large number of Syndecan-4+ cells are evident (Fig. 6E) that are β -galactosidase+ (Fig. 6F). A magnified 3D reconstruction from a confocal series shows a donor-derived satellite cell (Fig. 6G, caret) and two endogenous satellite cells (Fig. 6H, arrows) in re-injured muscle (Fig. 6I). We tested the capacity of the donor-derived satellite cells in re-injured *mdx^{4CV}* muscle to differentiate by explanting single myofibers, allowing the myofiber-associated cells to migrate off of the fiber into the culture dish. Donor-derived β -galactosidase+ cells differentiated and fused into multinucleated myotubes in culture (Fig. 6J–L), demonstrating the myogenic capacity of the satellite-SP cells following two successive rounds of muscle injury in the *mdx^{4CV}* mouse.

Discussion

We have identified a subset of resident myogenic stem cells distinct from the majority of the satellite cell population that exhibit unique characteristics consistent with that of a satellite cell progenitor population. These cells express the satellite cell markers Pax7, Syndecan-3 and Syndecan-4, the SP marker ABCG2 and Sca1. They can be found in muscle sections and remain tightly associated with myofibers upon isolation. Whether isolated by dye exclusion or FACS sorted these cells are capable of spontaneous differentiation into skeletal muscle. Unlike the majority of satellite cells, these cells possess an SP phenotype identified by Hoechst dye exclusion, express ABCG2 and comprise ~3–10% of the Syndecan-4+ population. When isolated, satellite-SP cells (Syndecan-4+/ABCG2+/Sca1+) exhibit a robust engraftment into the host satellite cell niche and generate myonuclear progeny that express muscle-specific genes. Moreover, upon re-injury, the contribution of donor-derived satellite-SP cells to the myonuclear and satellite cell compartments in re-injured muscle was equivalent or better than the initial engraftment, demonstrating the capacity of satellite-SP cells to renew the satellite cell pool. Whereas engraftment of CD34 enriched cells from muscle are capable of generating satellite cell progeny (Montarras et al., 2005; Cerletti et al., 2008; Sacco et al., 2008) satellite-SP cells are more efficient than any other reported cell type in generating satellite cell progeny when engrafted into host regenerating skeletal muscle. Moreover, satellite-SP cells appear capable of extensive self-renewal of the satellite cell pool *in vivo*, supporting our hypothesis that they function as satellite cell progenitors. Because these cells comprise a subpopulation of muscle SP cells we believe that they may account for the variable myogenic capacity previously observed in cultures of muscle-derived SP cells (Asakura et al., 2002; Gussoni et al., 1999) and the satellite cell progenitor capacity observed in CD34-enriched satellite cells (Montarras et al., 2005; Cerletti et al.,

2008; Sacco et al., 2008). Of particular interest is the observation that some of the skeletal muscle SP cells are somitically-derived (Schienda et al., 2006) and it remains to be determined if the satellite-SP cells arise from this population. We propose a model (Fig. 7) whereby satellite-SP cells function as myogenic progenitors or stem cells for the resident satellite cell population. Satellite-SP cells activate and divide to produce satellite cell progeny; we have not yet determined if satellite-SP cells constitute a distinct cell lineage or if a satellite-SP cell can arise from a main-population satellite cell that is present in a specialized niche. The behavior of the satellite-SP cells in intact myofiber cultures suggest that the factors controlling their cell cycle entry are distinct from those of the majority of satellite cells since they appear to cycle once and then either exit the cell cycle completely or cycle very slowly, a trait that has been ascribed to both stem cells in general and myogenic stem cells in particular (Shinin et al., 2006; Conboy et al., 2007). Future work is aimed at identifying the factors necessary for satellite-SP cell proliferation, determining whether these cells generate satellite cell progeny by an asymmetric division and identifying the source of satellite-SP cells.

Experimental Procedures

Mice

Mice were bred and housed according to NIH guidelines for the ethical treatment of animals in a pathogen-free facility at the University of Colorado. Wild type mice were C57Bl/6xDBA2 (B6D2F1; Jackson Labs); Rosa26 (B6;129S-*Gt(ROSA)26Sor*) (Zambrowicz, 1997) and *mdx*^{4CV} (Chapman et al., 1989) mice were obtained from Jackson Labs. *Abcg2/GFP* (Tadjali, 2006) mice were from Brian Sorrentino (St. Jude Children's Research Hospital). Cells or myofibers were harvested from female mice 3–6 months old.

Cells and myofibers

Bone marrow cells were flushed from femurs and resuspended at 10⁶ cells/ml in DMEM and 10% calf serum. Primary muscle cells were isolated from adult mouse hindlimb muscle. Briefly, muscle was digested with type I collagenase (Worthington), filtered and recovered in F12-C and 15% horse serum and 0.5nM FGF-2. SP cells were cultured in alpha-MEM media (Invitrogen) with 20% FBS and 0.5nM FGF-2. Unless otherwise noted myofibers and associated satellite cells were prepared as previously described (Cornelison et al., 2001) and either fixed immediately in 4% paraformaldehyde or cultured in F12-C and 15% horse serum and 0.5nM FGF-2. As required, BrdU, at 10 μ M (Sigma) was added.

FACS

For SP profiles bone marrow cells and primary muscle cells were processed as described (Goodell et al., 1996). Briefly, following isolation, cells were incubated 90min at 37°C in 5 μ g/ml (bone marrow) or 7.5 μ g/ml (muscle) Hoechst 33342 (Sigma). To delineate the SP gate, verapamil (Sigma) was added at a final concentration of 50 μ M. Profiles/sorts were generated on a MoFlo cell sorter (DakoCytomation). For antibody staining, cells were incubated for 45min at 4°C with primary antibodies (at 1:100 unless otherwise noted): mouse anti-ABCG2 (BCRP1) 5D3 (BD Pharmingen); mouse anti-ABCG2-PE (BCRP1) 5D3 (Chemicon); rat anti-CD45-FITC 30-F11 (BD Pharmingen); rat anti-Gr-1-Alexa488 RB6-8C5 (BoiLegend); rat anti-Mac-1-FITC M1/70 (Leinco Technologies); mouse anti-Pax7 (Developmental Studies Hybridoma Bank) conjugate to mouse Fc-PE-680 (Molecular Probes) at 1:5; rat anti-PECAM-FITC Mec13.3 (BD Pharmingen); rat anti-Sca1-FITC E13-161.7 (BD Pharmingen); rabbit anti-Syndecan-3 (Cornelison, 2001); chicken anti-Syndecan-4 (Cornelison, 2004) at 1:1500; rat anti-Thy-1-FITC 30-H12 (BioLegend). Secondary antibodies were (at 1:100 unless otherwise noted): anti-chicken-Alexa488 (Molecular Probes) 1:500; anti-chicken-PE (Open Biosystems); anti-mouseIgG-PE-Cy5

(Santa Cruz); anti-ratIgG-PE-Cy7 (Santa Cruz). Fluorescein diacetate (Sigma) was used at a final concentration of 2 μ g/ml. Caltat fix and perm was used for permeabilized cells. Profiles/sorts were generated using the MoFlo (DakoCytomation) or FACScan (BD Biosciences) with background gates set such that secondary antibodies alone, or isotype controls yielded less than 0.5% positive events.

Immunofluorescence

Cells, myofibers and sections were fixed in 4% paraformaldehyde. In addition to the primary antibodies listed above, rabbit anti- β -galactosidase (Abcam, 1:1000), rat anti-BrdU BUI/75 (Serotec, 1:100), rabbit anti-Dystrophin (Abcam, 1:200), rat anti-laminin 4HB-2 (Sigma, 1:200) and rabbit anti-laminin (Sigma, 1:200) were used. Additional secondary antibodies were: anti-chicken-Alexa594 or 647 (Molecular Probes); anti-chicken-AMCA (Jackson ImmunoResearch); anti-mouse-Alexa488 or 594 (Molecular Probes); anti-mouseIgG₁-FITC (SouthernBiotech); anti-mouseIgG_{2b}-Texas Red (SouthernBiotech); anti-rat-Alexa488, 594 or 647 (Molecular Probes); anti-rat-AMCA (Jackson ImmunoResearch); anti-rabbit-Alexa488, 594 or 647 (Molecular Probes) all at 1:100 except Alexa probes were at 1:500. Epifluorescent images were captured using a Nikon Eclipse E800 equipped with a Cooke Sencisam digital camera and deconvoluted using Slidebook software (Intelligent Imaging Innovations). Deconvoluted background fluorescence was subtracted from the primary signal. Individual tiff files were exported from Slidebook software. Confocal images and Z-series stacks were captured with a Leica TCS SP2 AOBS confocal microscope. Fluorescent images were processed with either Leica software or Volocity (Improvision) to process 3D reconstructions.

Microarray

Cells were isolated from mouse hindlimb muscle and sorted for Syndecan-3/Syndecan-4 expression as described above; source muscles were either uninjured or injected with 1.2% BaCl₂ 24hrs prior to harvest to induce myonecrosis (Caldwell et al., 1990). At least three independent age-matched animals were analyzed per time point. Total RNA was isolated using a PicoPure RNA Isolation Kit (Arcturus) followed by two rounds of linear T7-based amplification (RiboAmp HA Kit, Arcturus) for an RNA equivalent to 5000 dual-positive cells (based on the number of cells collected). Biotin-labeled antisense RNA was generated with IVT Labeling Kit (Affymetrix), and labeled cRNA was quantified and analyzed for size representation using a BioAnalyzer (Agilent). 5 μ g of labeled cRNA was fragmented and hybridized to Affymetrix 430 v.2 mouse microarrays at the University of Colorado Core facilities; chips were scanned on a GeneChip Scanner 3000 (Affymetrix) and intensity data recovered in GCOS (Affymetrix). CEL files from three replicate genechips were imported directly into Spotfire (TIBCO) and normalized by GCRMA. ANOVA analysis set at an FDR of 0.05% was used to identify differentially expressed probesets. Probesets with ≥ 2 -fold changes between uninjured and 24hr injured datasets were further identified by K-means and SOM clustering. Probesets with significant changes observed in satellite and stem cells were identified and plotted according to their relative expression.

Regeneration and cell transplants

To isolate cells from injured tissue, mice were anesthetized with isoflurane and tibialis anterior muscles were injected with 50 μ l 1.2% BaCl₂, followed with a 24hr recovery period. Muscles were processed for sorting and RNA extraction as described above. For transplantation studies, donor Syndecan-4+/ABCG2+/Sca1+ and Syndecan-4+/ABCG2-/Sca1- cells were isolated from hindlimb muscles of Rosa26 mice. Host B6D2F1 mice were anesthetized with isoflurane and tibialis anterior muscles were injected with donor cells in 50 μ l 1.2% BaCl₂ followed with recovery periods of 30 days. Muscle tissue was then harvested and processed for immunofluorescence as described above.

Supplementary Material

Refer to Web version on PubMed Central for supplementary material.

Acknowledgments

The authors would like to acknowledge Karen Helm at The University of Colorado Cancer Center Flow Cytometry Core (Supported by NIH P30CA046934) for assistance with cell isolation and Helen Marshall at the University of Colorado, MDC-Biology Department DNA Array Analysis Facility for Affymetrix hybridization and scanning. The authors have no commercial affiliations or conflict of interests. This work was supported by NIH AR39467, AR49446, and AG28907 to BBO; NIH 5T32HL007851 to KKT; Muscular Dystrophy Association Development Grant to DDWC; NIH GM066728-01 to JKH; APS Giles Filley Award and AHA-SDG0335032N to SMM.

References

- De Angelis L, Berghella L, Coletta M, Lattanzi L, Zanchi M, Cusella-De Angelis MG, Ponzetto C, Cossu G. Skeletal myogenic progenitors originating from embryonic dorsal aorta coexpress endothelial and myogenic markers and contribute to postnatal muscle growth and regeneration. *J Cell Biol.* 1999; 147:869–878. [PubMed: 10562287]
- Asakura A, Hirai H, Kablar B, Morita S, Ishibashi J, Piras BA, Christ AJ, Verma M, Vineretsky KA, Rudnicki MA. Increased survival of muscle stem cells lacking the MyoD gene after transplantation into regenerating skeletal muscle. *Proc Natl Acad Sci U S A.* 2007; 104:16552–57. [PubMed: 17940048]
- Asakura A, Seale P, Girgis-Gabardo A, Rudnicki MA. Myogenic specification of side population cells in skeletal muscle. *J Cell Biol.* 2002; 159:123–134. [PubMed: 12379804]
- Beauchamp JR, Morgan JE, Pagel CN, Partridge TA. Dynamics of myoblast transplantation reveal a discrete minority of precursors with stem cell-like properties as the myogenic source. *J Cell Biol.* 1999; 144:1113–122. [PubMed: 10087257]
- Bosnakovski D, Xu Z, Li W, Thet S, Cleaver O, Perlingeiro RC, Kyba M. Prospective Isolation of Skeletal Muscle Stem Cells With A Pax7 Reporter. *Stem Cells.* 2008
- Brack AS, Conboy MJ, Roy S, Lee M, Kuo CJ, Keller C, Rando TA. Increased Wnt signaling during aging alters muscle stem cell fate and increases fibrosis. *Science (New York, N Y).* 2007; 317:807–810.
- Caldwell CJ, Matthey DL, Weller RO. Role of the basement membrane in the regeneration of skeletal muscle. *Neuropathol Appl Neurobiol.* 1990; 16:225–238. [PubMed: 2402330]
- Cerletti M, Jurga S, Witczak CA, Hirshman MF, Shadrach JL, Goodyear LJ, Wagers AJ. Highly Efficient, Functional Engraftment of Skeletal Muscle Stem Cells in Dystrophic Muscles. *Cell.* 2008; 134:37–47. [PubMed: 18614009]
- Chapman VM, Miller DR, Armstrong D, Caskey CT. Recovery of induced mutations for X chromosome-linked muscular dystrophy in mice. *Proc Natl Acad Sci U S A.* 1989; 86:1292–96. [PubMed: 2919177]
- Conboy MJ, Karasov AO, Rando TA. High Incidence of Non-Random Template Strand Segregation and Asymmetric Fate Determination In Dividing Stem Cells and their Progeny. *PLoS Biol.* 2007; 5:e102. [PubMed: 17439301]
- Cornelison D, Filla MS, Stanley HM, Rapraeger AC, Olwin BB. Syndecan-3 and syndecan-4 specifically mark skeletal muscle satellite cells and are implicated in satellite cell maintenance and muscle regeneration. *Developmental Biology.* 2001; 239:79–94. [PubMed: 11784020]
- Dellavalle A, Sampaolesi M, Tonlorenzi R, Tagliafico E, Sacchetti B, Perani L, Innocenzi A, Galvez BG, Messina G, et al. Pericytes of human skeletal muscle are myogenic precursors distinct from satellite cells. *Nat Cell Biol.* 2007
- Goodell MA, Brose K, Paradis G, Conner AS, Mulligan RC. Isolation and functional properties of murine hematopoietic stem cells that are replicating in vivo. *J Exp Med.* 1996; 183:1797–1806. [PubMed: 8666936]

- Gussoni E, Soneoka Y, Strickland CD, Buzney EA, Khan MK, Flint AF, Kunkel LM, Mulligan RC. Dystrophin expression in the mdx mouse restored by stem cell transplantation. *Nature*. 1999; 401:390–94. [PubMed: 10517639]
- Jackson KA, Mi T, Goodell MA. Hematopoietic potential of stem cells isolated from murine skeletal muscle. *Proc Natl Acad Sci U S A*. 1999; 96:14482–86. [PubMed: 10588731]
- Kuang S, Kuroda K, Le Grand F, Rudnicki MA. Asymmetric self-renewal and commitment of satellite stem cells in muscle. *Cell*. 2007; 129:999–1010. [PubMed: 17540178]
- LaBarge MA, Blau HM. Biological progression from adult bone marrow to mononucleate muscle stem cell to multinucleate muscle fiber in response to injury. *Cell*. 2002; 111:589–601. [PubMed: 12437931]
- Majka SM, Beutz MA, Hagen M, Izzo AA, Voelkel N, Helm KM. Identification of novel resident pulmonary stem cells: form and function of the lung side population. *Stem Cells*. 2005; 23:1073–081. [PubMed: 15987674]
- Majka SM, Jackson KA, Kienstra KA, Majesky MW, Goodell MA, Hirschi KK. Distinct progenitor populations in skeletal muscle are bone marrow derived and exhibit different cell fates during vascular regeneration. *J Clin Invest*. 2003; 111:71–79. [PubMed: 12511590]
- Meeson AP, Hawke TJ, Graham S, Jiang N, Elterman J, Hutcheson K, Dimaio JM, Gallardo TD, Garry DJ. Cellular and molecular regulation of skeletal muscle side population cells. *Stem Cells*. 2004; 22:1305–320. [PubMed: 15579648]
- Mitchell PO, Mills T, O'Connor RS, Kline ER, Graubert T, Dzierzak E, Pavlath GK. Sca-1 negatively regulates proliferation and differentiation of muscle cells. *Dev Biol*. 2005; 283:240–252. [PubMed: 15901485]
- Montanaro F, Liadaki K, Schianda J, Flint A, Gussoni E, Kunkel LM. Demystifying SP cell purification: viability, yield, and phenotype are defined by isolation parameters. *Exp Cell Res*. 2004; 298:144–154. [PubMed: 15242769]
- Montarras D, Morgan J, Collins C, Relaix F, Zaffran S, Cumano A, Partridge T, Buckingham M. Direct isolation of satellite cells for skeletal muscle regeneration. *Science (New York, N Y)*. 2005; 309:2064–67.
- Muskiewicz KR, Frank NY, Flint AF, Gussoni E. Myogenic potential of muscle side and main population cells after intravenous injection into sub-lethally irradiated mdx mice. *J Histochem Cytochem*. 2005; 53:861–873. [PubMed: 15995145]
- Olguin HC, Olwin BB. Pax-7 up-regulation inhibits myogenesis and cell cycle progression in satellite cells: a potential mechanism for self-renewal. *Dev Biol*. 2004; 275:375–388. [PubMed: 15501225]
- Sacco A, Doyonnas R, Kraft P, Vitorovic S, Blau HM. Self-renewal and expansion of single transplanted muscle stem cells. *Nature*. 2008; 456:502–06. [PubMed: 18806774]
- Sampaolesi M, Blot S, D'Antona G, Granger N, Tonlorenzi R, Innocenzi A, Mognol P, Thibaud JL, Galvez BG, et al. Mesoangioblast stem cells ameliorate muscle function in dystrophic dogs. *Nature*. 2006; 444:574–79. [PubMed: 17108972]
- Sampaolesi M, Torrente Y, Innocenzi A, Tonlorenzi R, D'Antona G, Pellegrino MA, Barresi R, Bresolin N, De Angelis MG, et al. Cell therapy of alpha-sarcoglycan null dystrophic mice through intra-arterial delivery of mesoangioblasts. *Science*. 2003; 301:487–492. [PubMed: 12855815]
- Schianda J, Engleka KA, Jun S, Hansen MS, Epstein JA, Tabin CJ, Kunkel LM, Kardon G. Somitic origin of limb muscle satellite and side population cells. *Proc Natl Acad Sci U S A*. 2006; 103:945–950. [PubMed: 16418263]
- Schultz E. Satellite cell proliferative compartments in growing skeletal muscles. *Dev Biol*. 1996; 175:84–94. [PubMed: 8608871]
- Seale P, Sabourin LA, Girgis-Gabardo A, Mansouri A, Gruss P, Rudnicki MA. Pax7 is required for the specification of myogenic satellite cells. *Cell*. 2000; 102:777–786. [PubMed: 11030621]
- Shinin V, Gayraud-Morel B, Gomès D, Tajbakhsh S. Asymmetric division and cosegregation of template DNA strands in adult muscle satellite cells. *Nat Cell Biol*. 2006; 8:677–682. [PubMed: 16799552]
- Tadjali M, Zhou S, Rehg J, Sorrentino BP. Prospective isolation of murine hematopoietic stem cells by expression of an Abcg2/GFP allele. *Stem Cells*. 2006; 24:1556–563. [PubMed: 16484343]

- Zambrowicz BP, Imamoto A, Fiering S, Herzenberg LA, Kerr WG, Soriano P. Disruption of overlapping transcripts in the ROSA beta geo 26 gene trap strain leads to widespread expression of beta-galactosidase in mouse embryos and hematopoietic cells. *Proc Natl Acad Sci U S A*. 1997; 94:3789–794. [PubMed: 9108056]
- Zammit PS, Golding JP, Nagata Y, Hudon V, Partridge TA, Beauchamp JR. Muscle satellite cells adopt divergent fates: a mechanism for self-renewal? *J Cell Biol*. 2004; 166:347–357. [PubMed: 15277541]
- Zhou S, Schuetz JD, Bunting KD, Colapietro AM, Sampath J, Morris JJ, Lagutina I, Grosveld GC, Osawa M, et al. The ABC transporter Bcrp1/ABCG2 is expressed in a wide variety of stem cells and is a molecular determinant of the side-population phenotype. *Nat Med*. 2001; 7:1028–034. [PubMed: 11533706]

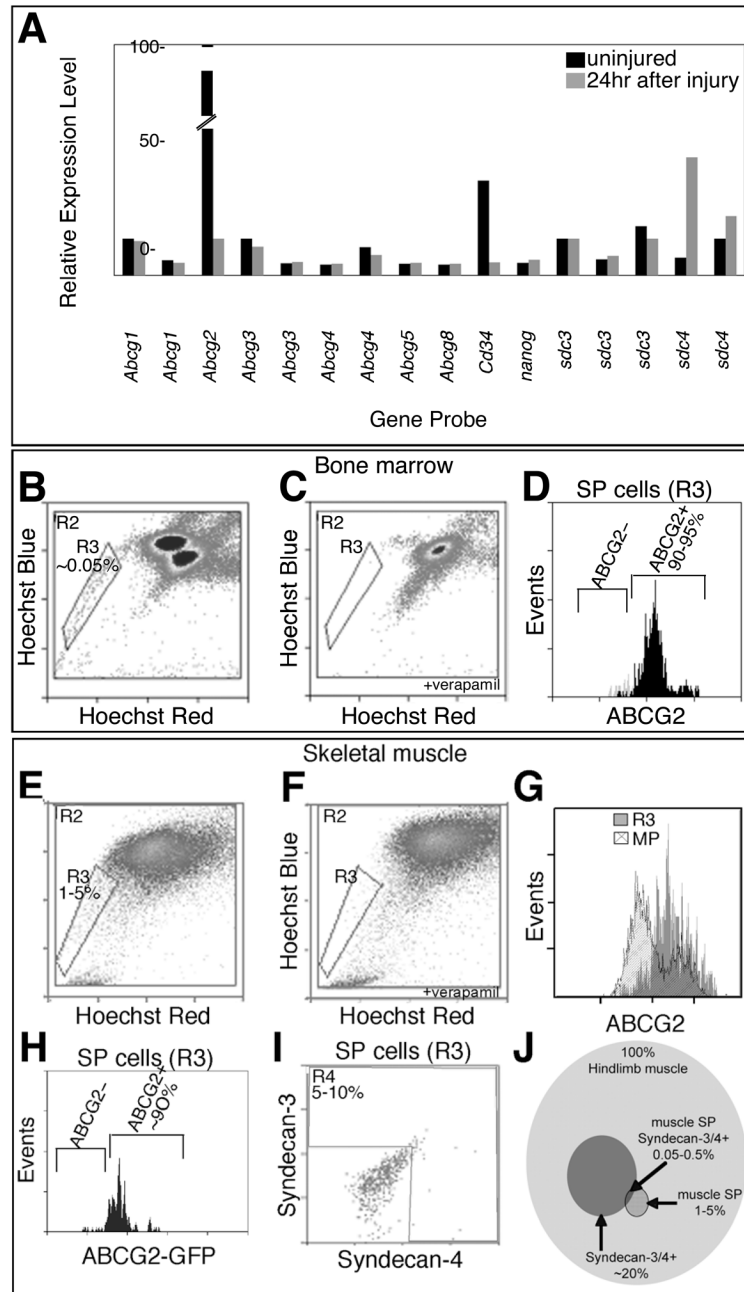


Figure 1. A subset of skeletal muscle SP cells express the satellite cell markers Syndecan-4 and Syndecan-3

Relative expression levels of genes obtained from microarray data from FACS purified Syndecan-3⁺/Syndecan-4⁺ satellite cells isolated from uninjured muscles (black) and muscles 24hr after BaCl₂ injury (grey) and filtered for selected stem cell genes: the *Abcg* family, *Cd34*, *nanog*, and the satellite cell-specific genes *sdc3* and *sdc4* (A, probesets ordered 5' to 3'). Live cell FACS profiles for bone marrow-derived cells (B–D) and skeletal muscle-derived cells (E–I) incubated with Hoescht 33342 in the presence (C, F) and absence (B, D, E, G–I) of verapamil to identify the SP gate (R3 regions with cell percentages noted). Greater than 90% of SP cells from both tissues express the ABCG2 transporter (D, G, grey histogram with ABCG2 antibody and H using the *Abcg2*/GFP

mouse (Tadjali et al., 2006)) while the majority of main population cells located above the SP gate do not express ABCG2 (**G**, hatched histogram). A subpopulation of muscle SP cells also expresses the satellite cell markers Syndecan-4 and Syndecan-3 (**I**, R4 region) as identified by co-staining with antibodies during SP profiling. (**J**) A Venn diagram depicting the percent of Syndecan-3+/Syndecan-4+ muscle SP cells within the cohort of all cells in the entire hindlimb muscle tissue and within the context of muscle SP cells. Percentages of individual cell populations are noted. Background gates were set with less than 0.5% of controls scored as positive.

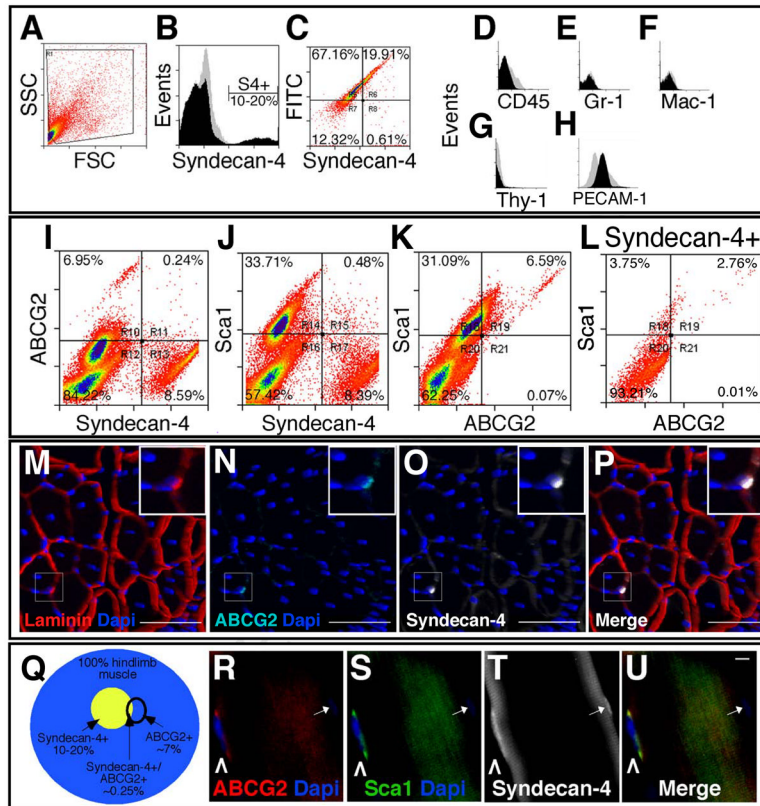


Figure 2. Satellite-SP cells express the stem cell markers ABCG2 and Sca1

Live cell FACS profiles for hindlimb skeletal muscle (A–L) identify a population of Syndecan-4+ satellite cells in the total events (A, FSC/forward scatter and SSC/side scatter), plotted as events vs. Syndecan-4 fluorescence intensity to resolve Syndecan-4+ cells (B, black profile) from background (B, grey profile). Live cells convert fluorescein diacetate to FITC showing the majority of Syndecan-4+ cells are viable (C, region R6). Syndecan-4+ cells are negative for the blood lineage markers CD45 (D), Gr-1 (E), Mac-1 (F) and Thy-1 (G) and 7% Syndecan4+ cells express PECAM-1 (H). Profiling simultaneously for three markers on live cells we identified a subset of Syndecan-4+ cells that express the stem cell markers ABCG2 (I, R11) and Sca1 (J, R15). Approximately 7% of the hindlimb muscle-derived cells express both ABCG2 and Sca1 (K, R19) and this subset of ABCG2+/Sca1+ cells represents ~3% of Syndecan-4+ cells (L, R19). A satellite-SP cell (inset in M–P) in a 3D reconstruction of muscle section from a confocal Z-series is located underneath the basal lamina (M, red) and immunoreactive for ABCG2 (N, P, cyan) and Syndecan-4 (O, P, white). The inset (M–P) is a magnified region of the boxed area. (Q) A Venn diagram depicting the percentage of Syndecan-4+, ABCG2+ and dual positive cells represented in collagenase digested hindlimb muscle. Freshly isolated myofibers retain rare satellite-SP cells R–U, caret) immunoreactive for ABCG2 (R, red, caret), Sca1 (S, green, caret), and Syndecan-4 (T, white, caret); DNA is counterstained with DAPI (R, S, U, blue). In addition, note the ABCG2 negative Syndecan-4+ satellite cell on this fiber (R–U, arrow) where DAPI is not bright in this plane of focus. In B, D–H black histograms represent specific antibody immunoreactivity and grey histograms are the corresponding control. In A–L, all gates were determined by setting controls at less than 0.5% positive events. For M–P the scale bar represents 75µm and for R–U 1µm.

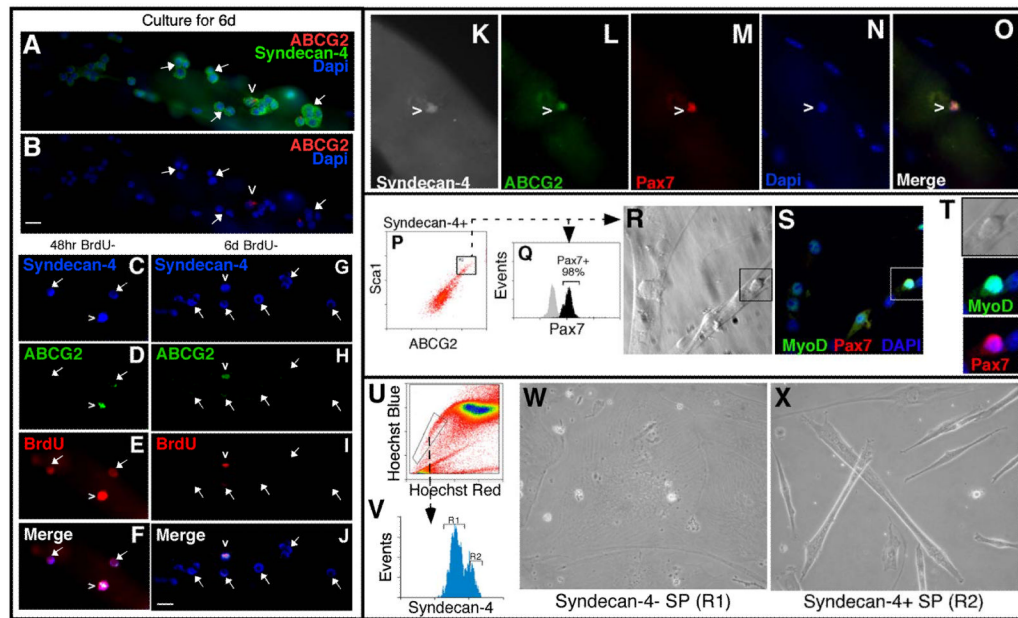


Figure 3. Satellite-SP cells express Pax7 and exhibit distinct behaviors in culture

Myofibers cultured for 6 days (A, B) retain single rare ABCG2⁺/Syndecan-4⁺ (red and green respectively) satellite-SP cells (caret) surrounded by clusters of ABCG2⁻/Syndecan-4⁺ satellite cells (arrows mark some of the ABCG2⁻/Syndecan-4⁺ satellite cells). Following a 48hr BrdU pulse and 48hr chase, all satellite-SP cells (C–F, caret) and satellite cells (C–F, arrows) are BrdU positive (red) (C–F, Syndecan-4 (blue) and ABCG2 (green)). After a 6-day chase (G–J), only ABCG2⁺ satellite-SP cells (caret) retain BrdU (red) while satellite cells (arrows) are BrdU negative. Freshly isolated myofibers possess satellite-SP cells (caret in K–O) expressing Pax7 (M, red) in addition to Syndecan-4 (K, white) and ABCG2 (L, green). FACS sorted satellite-SP cells (P) were either fixed and permeabilized demonstrating that all satellite-SP (Syndecan-4⁺/ABCG2⁺/Sca1⁺) cells are Pax7⁺ (Q, black histogram) or cultured for 5d, fixed and visualized for myotubes (R) and stained for MyoD (S, green) and Pax7 (T, red). Boxed region in R and S identifies an unfused MyoD⁺/Pax7⁺ cell (T, inset). Sorting muscle SP cells by Hoescht dye exclusion (U) for Syndecan-4 immunoreactivity (V, R1 Syndecan-4⁻ and R2 Syndecan-4⁺ muscle SP cells) followed by 3 weeks in culture (W, X) revealed that only Syndecan-4⁺ satellite-SP (V, R2) cells spontaneously differentiated into myotubes (X). In T, the black histogram represents specific antibody immunoreactivity and the grey histogram is the corresponding control. Scale bars represent 10 μ m.

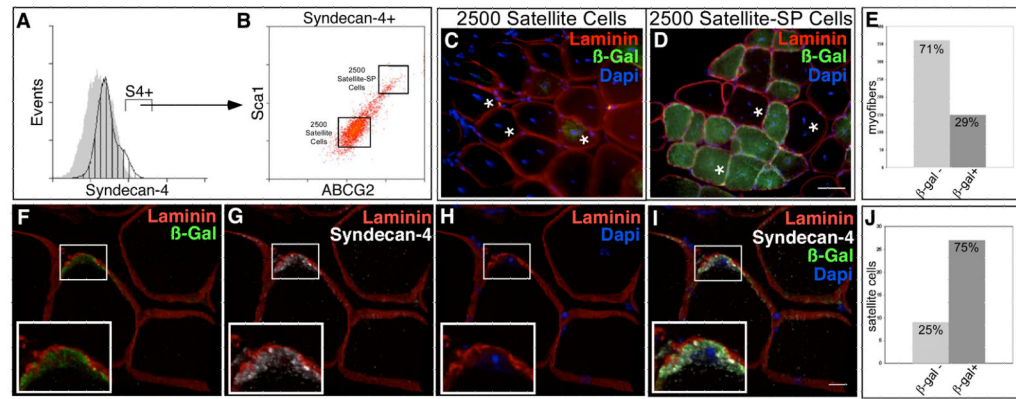


Figure 4. Satellite-SP cells engraft into myofibers and the satellite cell position *in vivo*
 Hindlimb skeletal muscle from Rosa26 mice was sorted for satellite-SP cells (A, Syndecan-4+, B, Syndecan-4+/ABCG2+/Sca1+, top box) or satellite cells (A, Syndecan-4+, B, Syndecan-4+/ABCG2-/Sca1-, bottom box) and 2500 cells were transplanted into regenerating tibialis anterior muscle of different host mice with 1.2% BaCl₂. (C, D) Representative epifluorescent images from cross sections of transplanted and injured muscle depicting the absence of β -galactosidase-expressing myofibers with transplantation of 2500 satellite cells (C) and β -galactosidase+ myofibers in satellite-SP cell transplanted tissue (D) 30 days after regeneration (asterisks mark centrally located nuclei). Scoring for donor derived β -galactosidase+ myofibers (E) following satellite-SP cell transplantation. (F–I) 3D reconstruction of confocal images of donor derived β -galactosidase+ (F, I, green) satellite cells 30 days after transplantation of satellite-SP cells (F–I, Laminin red; G, I, Syndecan-4 white; H, I, DAPI blue) with concurrent injury; insets are boxed. Scoring for donor derived β -galactosidase+ satellite cells (J) 30 days after transplantation of satellite-SP cells. In A, hatched histogram represents Syndecan-4 and grey histogram is the control; Syndecan-4+ (S4+) cells marked by bar. Scale bar in D represents 25 μ m and in I represents 10 μ m.

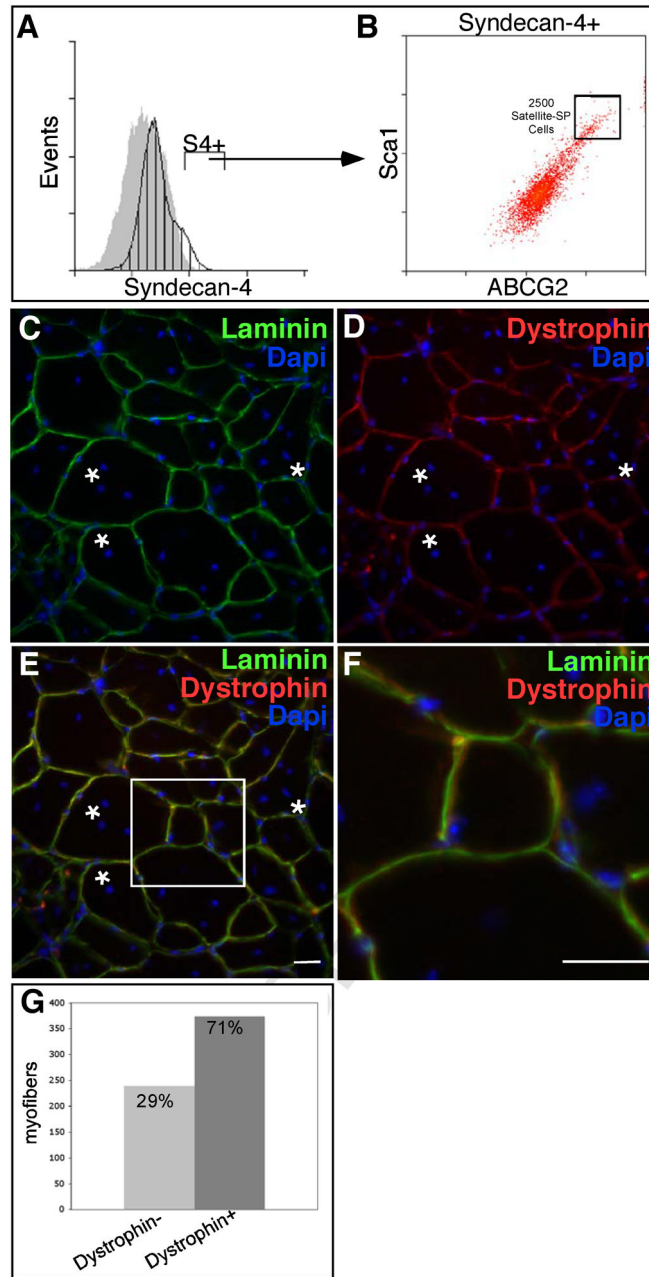


Figure 5. Satellite-SP cells generate Dystrophin+ fibers following transplantation Hindlimb skeletal muscle from Rosa26 mice was sorted for satellite-SP cells (**A**, Syndecan-4+, **B**, Syndecan-4+/ABCG2+/Sca1+, box) and transplanted into tibialis anterior muscles of *mdx*^{Acv} mice in the presence of 1.2% BaCl₂ to induce injury. (**C–F**) Representative epifluorescent images 30 days following transplantation and injury depicting centrally located nuclei (asterisks) and Dystrophin+ fibers (**D–F**, red). Scoring for Dystrophin+ fibers (**G**) 30 days following transplantation of satellite-SP cells.

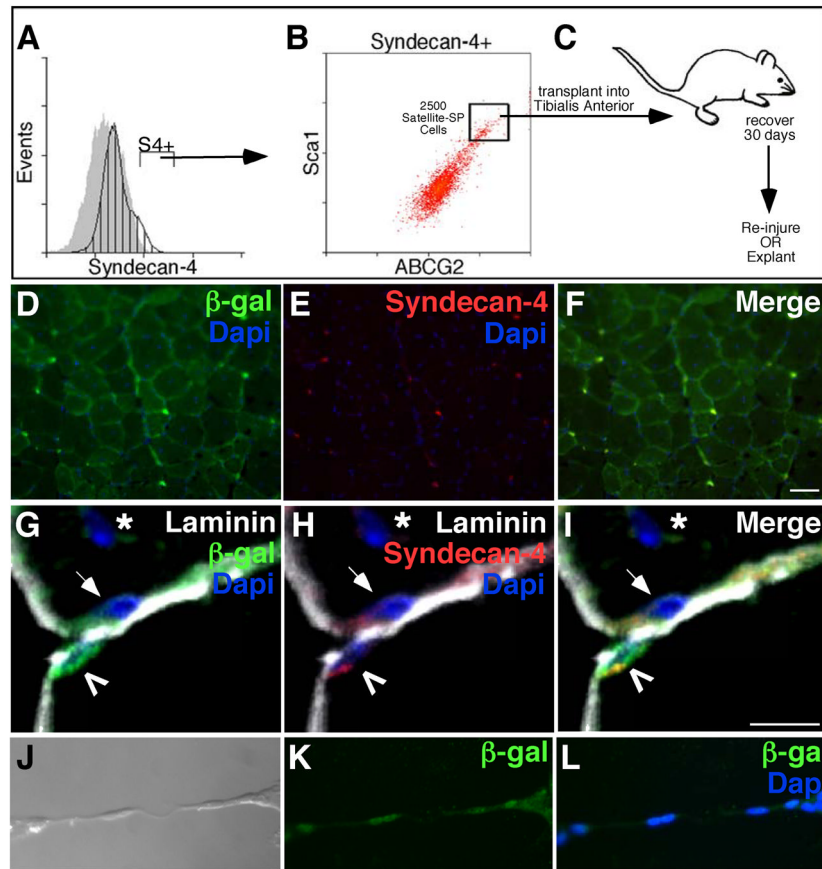


Figure 6. Transplanted Satellite-SP cells are found after multiple rounds of regeneration and are myogenic *in vitro*

Satellite-SP cells (A, Syndecan-4+, B, Syndecan-4+/ABCG2+/Sca1+ were isolated from hindlimb skeletal muscle of Rosa26 mice and transplanted into *mdx*^{4cv} tibialis anterior muscle. Following 30 days of regeneration, muscle was either re-injured with 1.2% BaCl₂, or explanted to isolate myofibers (C). (D–F) Representative epifluorescent images of re-injured tissue with continued presence of donor derived (β-galactosidase+, green D, F) Syndecan-4+ (red E, F) satellite cells. (G–I) 3D reconstruction of confocal images of donor derived (β-galactosidase+, green) Syndecan-4+ (red) cells located beneath the basal lamina (Laminin, white) 30 days following re-injury. Transplanted muscle fibers were explanted, satellite cells cultured and allowed to differentiate. Donor derived, β-galactosidase+ (green K, L) cells formed myotubes.

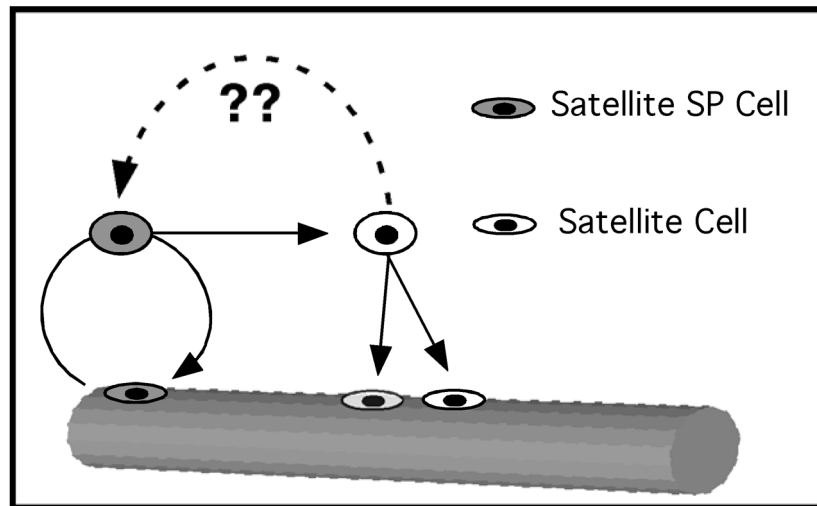


Figure 7. Satellite-SP cells self-renew and generate satellite cell progeny

Satellite-SP cells (grey) may divide asymmetrically to produce a satellite-SP cell and a satellite cell. Satellite cells are capable of symmetric division to produce satellite cell progeny. It is not known if satellite-SP cells constitute a lineage or arise from the interaction of a satellite cell with a specialized niche.